REVIEW ARTICLE

ZUO Liang, ZHANG Yu-dong, ZHAO Xiang, HE Chang-shu, CLAUDE Esling

Effects of High Magnetic Fields on the Microstructure Formation in a 42CrMo Steel During Solid Phase Transformations

Abstract This paper summarizes our recent work on the application of high static magnetic fields to the austenite-to-ferrite transformation and the tempering processes in hot-rolled 42CrMo steel. The thermodynamic and kinetic effects of the high magnetic fields on austenite decomposition and the influences of the high magnetic field on carbide precipitation and the matrix recovery during high- and low-temperature tempering are briefly outlined. Insight into these aspects may provide better understanding of the effects of high magnetic fields on diffusional phase transformations and is of both theoretical significance and technical interest.

1 Introduction

The introduction of magnetic field to solid-state phase transformations in steels has been a subject of active research for many years. If the parent and product phases are different in their saturation magnetization and are allowed to transform under a magnetic field, the transformation temperature and transformed amount can be considerably affected, as the Gibbs free energy of a phase can be lowered by an amount according to its magnetization. This effect has been first investigated theoretically and experimentally on several ferroalloys during their non-diffusional martensitic transformations [1–14]. Quite recently, attention shifted to the high-temperature diffusional transformations in high magnetic fields. Research on this topic is mainly concentrated on what follows (1) theoretical simulations of the effects of magnetic field on ferrite/austenite and austenite/ferrite phase equilibrium [15,16], (2) morphological features appearing during ferrite-to-austenite [17] and austenite-to-ferrite [18–20] transformations, and (3) kinetic characteristics of proeutectoid ferrite transformation under high magnetic field [21–23]. Some valuable information has been obtained and possible influential mechanisms have been proposed. The present authors have dealt with this topic extensively from both theoretical and experimental aspects. The main results in revealing the effects of high static magnetic fields on the austenitic decomposition and tempering behaviors of a medium carbon steel are summarized in this paper.

ZUO Liang (✉), ZHANG Yu-dong,
ZHAO Xiang, HE Chang-shu
Liaoning Key Laboratory of Microstructure Design
and Control of Metallic Materials,
Northeastern University,
Shenyang 110004, China
E-mail: lzuo@mail.neu.edu.cn

CLAUDE Esling
LETAM, CNRS-UMR 7078,
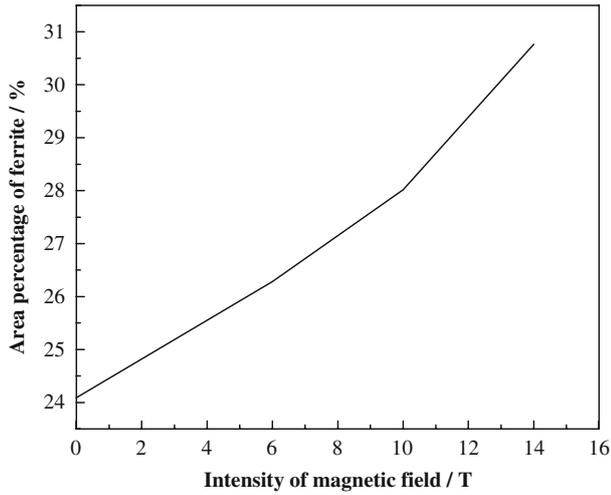University of Metz,
Ile du Saulcy,
57045 Metz, France

2 Ferritic and pearlitic transformation under high magnetic fields

Magnetic field (6, 10, and 14 T, respectively) was introduced when hot-rolled and fully austenitized (880°C×33 min) 42CrMo steel was cooled at 10 and 46°C/min, [24–30]. The magnetic field direction (MD) was kept in parallel to the hot-rolling direction (RD) for all the tested specimens. The application of high magnetic fields showed strong thermodynamic and kinetic effects on the austenite decomposition under these two cooling conditions.

2.1 Thermodynamic characteristics

The variations of the area percentage of ferrite with the intensity of magnetic field in specimens cooled at the rate of 10°C/min are shown in Fig. 1 [24]. It can be seen that the amount of ferrite increases with the increasing magnetic field. Indeed, the magnetic fields can impose considerable influence on the austenite/ferrite equilibrium and shift its boundary line (Ae_3 line) to the high-carbon concentration

Fig. 1 Influence of magnetic field on the amount of ferrite [24]

Fig. 3 Temperature variations of $\frac{\Delta G^M}{\Delta G_v + \Delta G^M}$ under 14-T magnetic field [24]

side [25]. As a result, the "$\alpha + \gamma$" area is enlarged and the eutectoid point moves to the high-carbon side in the Fe–C phase diagram. According to the "Level Law," one may deduce that the amount of the transformed proeutectoid ferrite is increased by the applied magnetic field. Therefore, the influence of a magnetic field on the phase equilibrium leads to an increase in the amount of ferrite.

2.2 Kinetic characteristics

The microstructures obtained under a cooling rate of 46°C/min without and with a 14-T magnetic field are shown in Fig. 2 [24]. In the nonmagnetic cooling case, the resulting microstructure (Fig. 2a) is mainly composed of bainite, with a slight amount of ferrite (bright areas), whereas the final microstructure (Fig. 2b) obtained with a 14-T field remains ferritic (bright areas) and pearlitic (dark areas).

The kinetic equation of the proeutectoid ferritic transformation from austenite decomposition reads [31]

$$\ln t = A \ln \left(\ln \frac{1}{1-f} \right) + B \frac{Q}{RT} + C \frac{\sigma^3}{\Delta G_v^2} - E \ln \frac{x^\gamma - x}{x^\gamma - x^\alpha} \tag{1}$$

where A, B, C, and E are constants; t is the transformation time of ferrite; Q, R, and T are the activation energy for diffusion, the gas constant, and the absolute temperature, respectively; σ and ΔG_v are the interfacial energy and the Gibbs volume free energy difference between the product and the parent phases, respectively; x^γ and x^α are the solubilities of austenite and ferrite at T; and x is the carbon content of the initial austenite. When a magnetic field is introduced, the third item in Eq. (1) is replaced by $C \frac{\sigma^3}{(\Delta G_v + \Delta G^M)^2}$, where ΔG^M is the Gibbs free energy difference between the product ferrite and the parent austenite lowered by the magnetic field. The proportional ratio of ΔG^M to $\Delta G^M + \Delta G_v$ (the total Gibbs free energy difference between the two phases in the magnetic field) is calculated and shown in Fig. 3 [24].

It can be seen from Fig. 3 that ΔG^M—as compared with $\Delta G^M + \Delta G_v$—is large enough within the whole temperature range of transformation, especially at higher temperatures, and thus, it can greatly reduce the incubation time of the austenite-to-ferrite transformation. Consequently, even at the higher cooling rate of 46°C/min, the holding time at the proeutectoid and eutectoid transformation temperature ranges is long enough in the high magnetic field to allow ferrite and pearlite to form, and therefore, the high-

Fig. 2 Microstructures of 42CrMo austenitized at 880°C for 33 min and cooled at 46°C/min without (**a**) and with (**b**) a 14-T magnetic field (MD is vertical in the picture) [24]
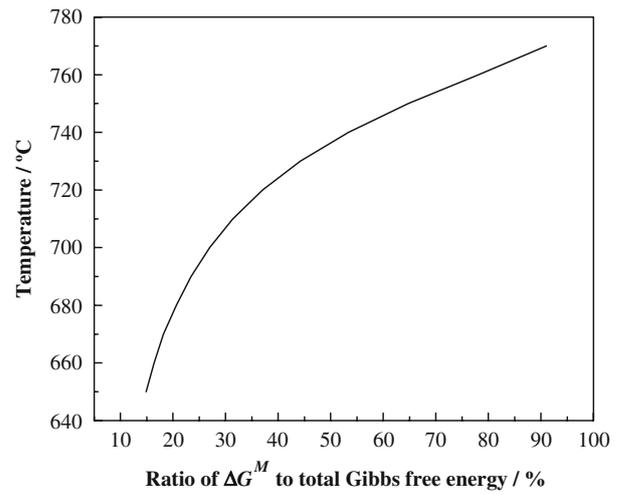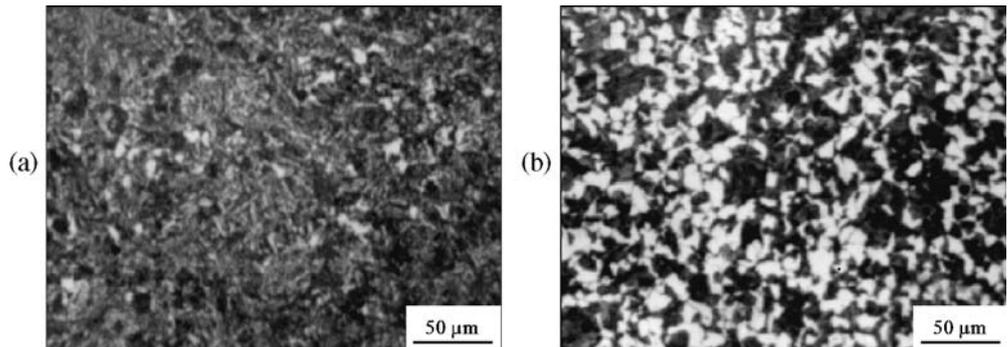
temperature equilibrium microstructure of ferrite and pearlite is obtained (Fig. 2b).

Based on these results, a rapid full annealing method is proposed [26]. For comparison, conventional annealing of the same material was performed at 860°C for 20 min and cooled down within the furnace at about 1°C/min. The microstructure obtained is shown in Fig. 4 [26]. It can be seen that ferrite grains and pearlite colonies aligned alternately along the previous RD, which is the typical banded structure. The original austenite grain structure after hot rolling is also shown in Fig. 5 [26].

It is evident in Fig. 5 that fine- and coarse-grained zones are alternately distributed along the RD. This can be attributed to the inhomogeneous deformation occurring in the hot-rolling stage and, in turn, results in the formation of the banded structure during subsequent annealing. This kind of microstructure is detrimental as it creates aniso-tropy in material performance and, therefore, should be avoided. To eliminate it, one usually applies a normalizing process. However, it always yields a bainitic or martensitic microstructure that is high in hardness and unfavorable to machining. Hence, an additional high-temperature temper-ing treatment is indispensable. In this connection, such a method is not economical in furnace batches and is rather complicated in operation.

Nevertheless, a so-called rapid full annealing approach in high magnetic field could offer a potential alternative. As can be seen in Fig. 2b, when the material is fully austenitized at 880°C and then rapidly cooled at 46°C/min in a 14-T magnetic field, the microstructure is still composed of ferrite and pearlite, but they are distributed randomly and the mean sizes of ferrite grains and pearlite colonies are smaller than those obtained by conventional annealing. Image analysis has shown that the area per-centages of ferrite obtained by rapid annealing in the 14-T magnetic field and by conventional annealing are 23.1% and 24.4%, respectively [26], which are very close to each other. In addition, the hardness of the specimens rapidly annealed in the 14-T magnetic field ranges within 192–210 HB [26], which lies just within the optimum hardness range of 160–230 HB for machining. Thus, the micro-
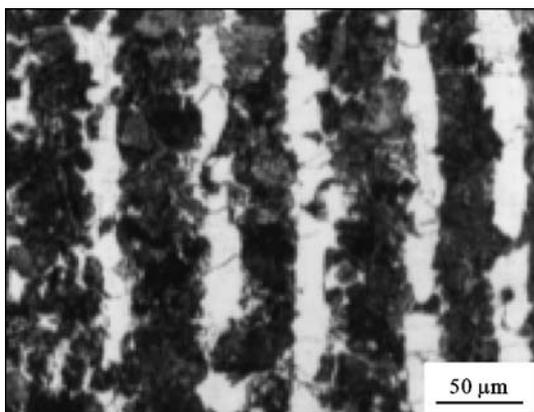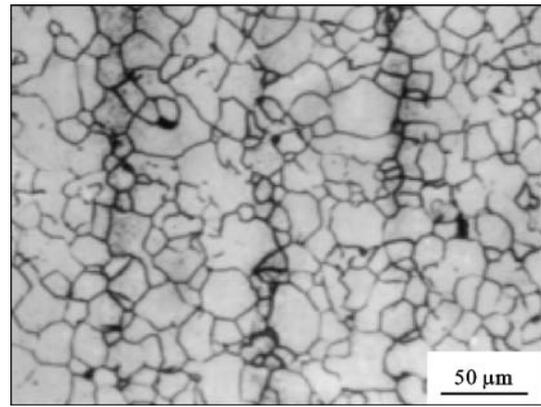

Fig. 5 Original austenite grain structure of 42CrMo after hot rolling (RD is vertical in the picture) [26]

structure and hardness of specimens rapidly annealed in the magnetic field fully meet the technical requirements.

In consequence, rapid annealing under a 14-T magnetic field has the following advantages: (1) improving micro-structure by avoiding banded structure and refining grains; (2) enhancing process efficiency through greatly short-ening the cooling time (45 times shorter) and leaving out additional heat treatments to eliminate the banded struc-ture. Hence, this may offer a promising approach to updating conventional processes.

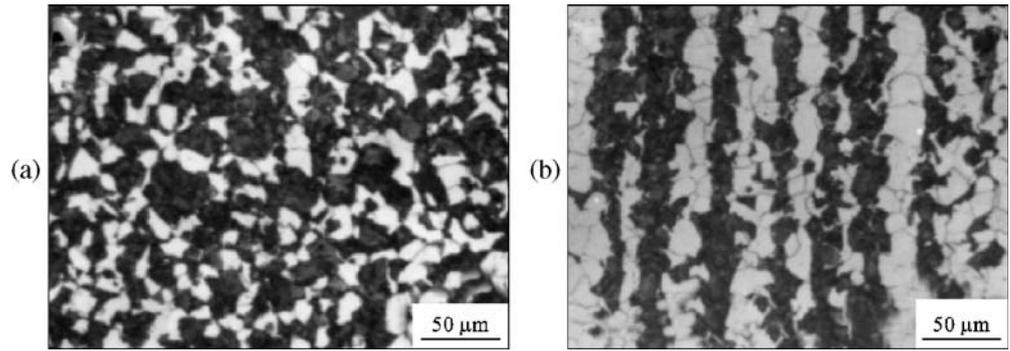## 2.3 Microstructural characteristics

The external high magnetic field can also exert significant influence on the microstructure formation. Figure 6 shows the microstructures of the specimens fully austenitized and cooled at 10°C/min without and with a 14-T magnetic field [27].

It can be seen that in both cases, the microstructures are composed of ferrite grains and pearlite colonies that are nearly equiaxed with basically uniform sizes. The only dif-ference is in their distribution. In Fig. 6a, only a few ferrite grains and pearlite colonies align along the RD, but most of them are distributed randomly. However, in Fig. 6b, it is interesting to see that they tend to align to the direction of the applied magnetic field. Microstructural observation has also shown that such a tendency becomes stronger with the increasing magnetic field [27]. Crystallographic orientation analysis by electron backscatter diffraction (EBSD) re-vealed that no preferential orientations exist in these ferrite chains [27], although the easy magnetization directions of ferrite are <100>.

For the phase transformation from austenite to ferrite, the nucleation rate can be expressed as

Fig. 4 Banded microstructure of 42CrMo after conventional annealing (RD is vertical in the picture) [26]

$$\dot{N} = N_0 \exp\left(-\frac{Q}{RT}\right) \exp\left(-\frac{\Delta G^*}{RT}\right) \qquad (2)$$

Fig. 6 Microstructures of 42CrMo austenitized at 880°C for 33 min and cooled at 10°C/min without (**a**) and with (**b**) a 14-T magnetic field (MD is vertical in the picture) [27]

where N_0 is a constant. The nucleation barrier ΔG^* reads

$$\Delta G^* = C \frac{\sigma^3}{\Delta G_v^2} \tag{3}$$

ΔG_v is strongly temperature dependent and increases rapidly with the decreasing temperature. The nucleation of ferrite needs the contribution of the diffusion and nucleation barrier terms in Eq. (2). However, they are always in a conflicting state. The diffusion term favors high-temperature nucleation because of the easiness in atom diffusion, but then, the nucleation barrier is high as ΔG_v is small and cannot counterbalance the increase in σ. As opposed to this, the nucleation barrier term favors nucleation at low temperature due to the low nucleation barrier, but then, atom diffusion becomes slow. Thus, through changing the nucleation sites, there would exist a compromise. When nucleation occurs at high temperature with a slow cooling rate, grain boundaries of the parent phase, especially triple boundaries, become the main nucleation sites for the new phase to form. The energy increase due to the creation of new interfaces between the product and parent phases can be lowered via the consumption of the grain boundary energy. In this case, if the original austenite grain size is not homogeneous, it could affect the distribution of the product phase. The fine austenite grain zones in Fig. 5 are considered to offer more nucleation sites than the coarse grain zones do. Finally, there yields a banded structure, as observed when cooling at 1°C/min (Fig. 4). If nucleation happens at a relatively low temperature with a fast cooling
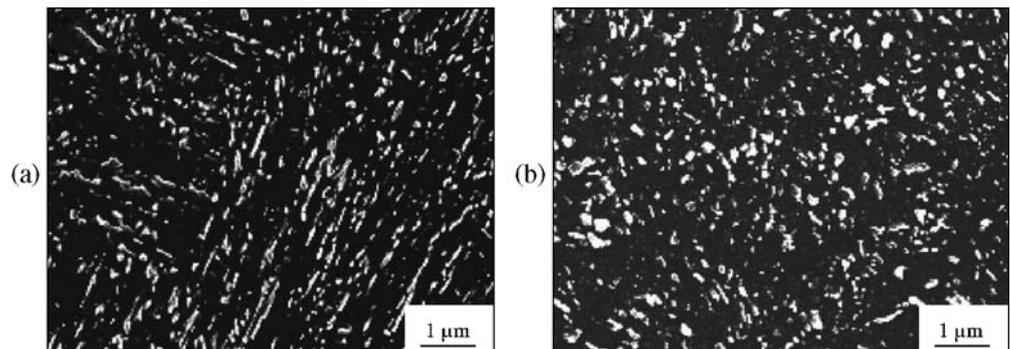
rate, the nucleation barrier is small owing to a relatively large ΔG_v. Hence, nuclei form not only along parent phase boundaries but also at energy undulating sites inside parent grains. Thus, the effect of the inhomogeneity in the original austenite grain structure is greatly reduced and the resultant microstructure with randomly distributed product phases might be obtained, as is the case when cooling at 10°C/min (Fig. 6a).

When a high magnetic field is applied, transformation can be greatly accelerated, as already discussed in Section 2.2. The keeping time, despite fast cooling, is long enough to allow ferrite to nucleate at higher temperatures. Hence, the application of a high magnetic field is equivalent to a decrease in cooling rate. In consequence, a banded microstructure may form at the relatively fast cooling rate of 10°C/min with a 14-T magnetic field (Fig. 6b), which is similar to that obtained at 1°C/min without the magnetic field.

3 Tempering behaviors under a high magnetic field

Quite recently, we have initiated the study of the tempering behaviors of steels under a high magnetic field. A 14-T magnetic field was applied to both high-temperature tempering (650°C×60 min) [28] and low-temperature tempering (200°C×60 min) [29] of hot-rolled 42CrMo steel after it was water-quenched from austenite state (860°C×20 min). It has been found that the magnetic field affects both the high- and low-temperature behaviors of the quenched material.

Fig. 7 SEM secondary electron images of carbide precipitates (bright areas) within martensite in 42CrMo tempered at 650°C for 60 min without (**a**) and with (**b**) a 14-T magnetic field (MD is vertical in the picture) [28]
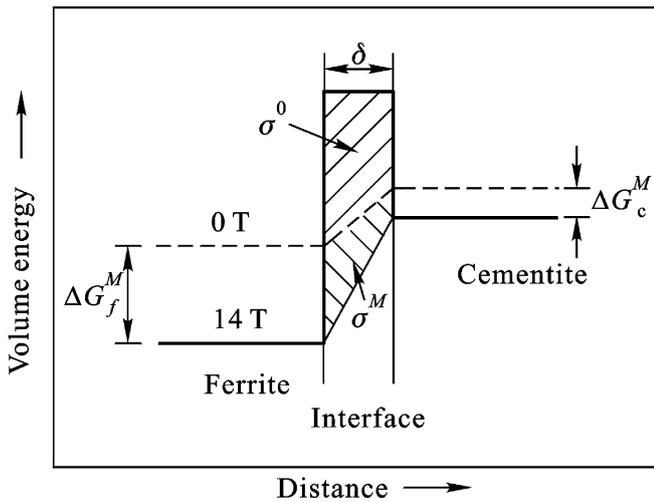
Fig. 8 Schematic illustration of cementite/ferrite interfacial energy without and with a magnetic field [28]

3.1 High-temperature tempering behaviors

3.1.1 Precipitation

For high-temperature tempering without or with a 14-T magnetic field, the cementite precipitates from the martensite matrix, as shown in Fig. 7 [28].

It can be seen that without the magnetic field, most of the cementite precipitates are long strips along the martensite plate boundaries and twin boundaries, while with the magnetic field, they remain sphere or particle a like. This suggests that the magnetic field can effectively prevent the directional growth of cementite precipitates. As both ferrite and cementite can be magnetized to some extent, their Gibbs free energies are lowered by the magnetic field. Since an interface between these two phases is highly disordered, its energy level remains almost unchanged. Consequently, the relative interfacial energy increases with the applied magnetic field, as schematically illustrated in Fig. 8 [28]. Thus, the shape of cementite becomes essential to minimize the final total interfacial energy. Obviously, the sphere- or particle-like cementite is most favorable. In addition, the magnetostrictions of cementite and ferrite are also different. When the hard cementite grows within the soft ferrite matrix, the directional growth of cementite would cause a large increase in strain energy [32], and thus it is not favored. Under these two effects of the magnetic field, the particle-like cementite that has minimum total interfacial area and minimum magnetostriction strain energy is most energetically favorable for its formation.

3.1.2 Recovery

When the oversaturated carbon atoms diffuse out from the matrix to form precipitates, the matrix gains the ability to recover its lattice distortion. Figure 9 shows the orientation maps of the specimens tempered at 650°C without and with a 14-T magnetic field, respectively [28].

In Fig. 9, the black areas represent the "distortion-free" regions and the remaining parts in gray are the "distorted" ones. Further analysis has shown that, for the specimens treated without and with the magnetic field, the percentages of the distortion-free regions are 7.24% and 5.42% in area and 55.41% and 51.64% in number, respectively. This indicates that the magnetic field has an obvious retardation effect on the formation and growth of the distortion-free regions. Indeed, a high magnetic field may lower the mobility of grain boundaries, either by atomic diffusion through magnetic ordering or by the obstructive effect of domain walls [33]. As the formation and growth of the distortion-free regions need atom diffusion and boundary migration, the recovery could be retarded by the application of the magnetic field.

3.2 Low-temperature tempering behaviors

In low-temperature tempering, the main microstructural change is the precipitation of transition carbides. They are metastable at different temperatures and change their forms when tempering temperature rises [34]. For the specimens tempered at 200°C for 60 min without and with a 14-T magnetic field, carbides have precipitated within martensite plates (Fig. 10) [29]. It can be seen that with the magnetic field, they are distributed more densely and with smaller sizes. The crystal structure of the precipitates and their orientation relationships with the matrix have been

Fig. 9 Orientation imaging microscopy (OIM) maps of 42CrMo tempered at 650°C for 60 min without (**a**) and with (**b**) a 14-T magnetic field (MD is horizontal in the picture) [28]
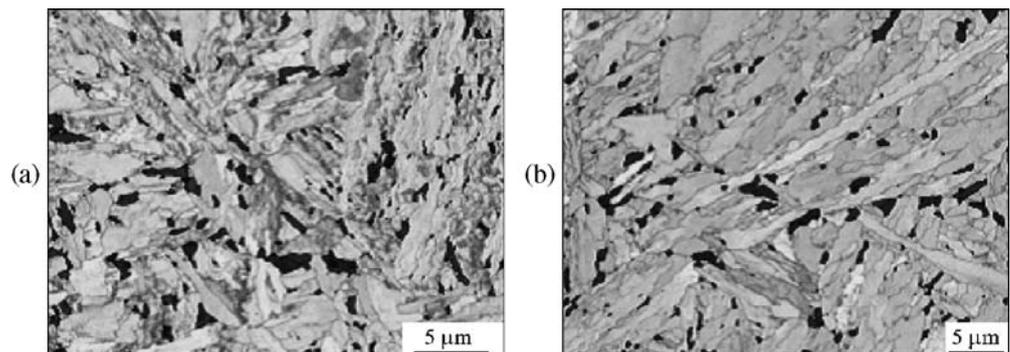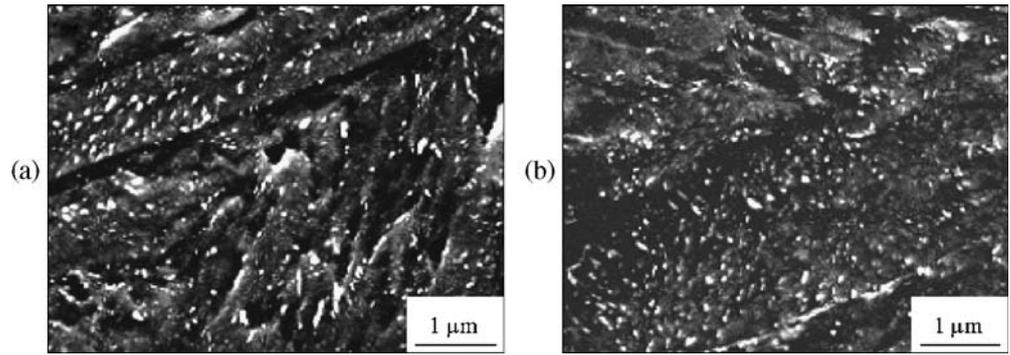
Fig. 10 SEM secondary electron images of carbide precipitates (bright areas) within martensite in 42CrMo tempered at 200°C for 60 min without (**a**) and with (**b**) a 14-T magnetic field (MD is vertical in the picture) [29]

identified by electron diffraction in TEM. The carbide formed during nonmagnetic tempering is of the typical orthorhombic η-Fe$_2$C and is correlated to the tempered martensite α'' by $(110)\alpha''//(200)\eta$ and $[1\,\overline{1}\,\overline{3}]\alpha''//[0\overline{2}0]\eta$, whereas in magnetic tempering, it is referred to as the monoclinic χ-Fe$_5$C$_2$ with the orientation correlation of $(01\overline{1})\alpha''//(021)\chi$ and $[1\overline{3}\,\overline{3}]\alpha''//[5\overline{3}6]\chi$ [29]. Normally,

Fig. 11 Temperature variations of magnetization of Fe$_2$C, Fe$_5$C$_2$, and α-Fe [29]

Fig. 12 Schematic diagram of Gibbs free energy vs carbon concentration for α' martensite, χ-Fe$_5$C$_2$, and η-Fe$_2$C at 200°C without (*dashed line*) or with (*solid line*) a 14-T magnetic field [29]

χ-Fe$_5$C$_2$ precipitates at higher temperatures after η-Fe$_2$C dissolves. Therefore, the magnetic field has an obvious effect on changing the precipitation sequence by skipping the precipitation of η-Fe$_2$C carbide.

It is known that η-Fe$_2$C and χ-Fe$_5$C$_2$ are both ferromagnetic at 200°C. From a thermodynamic point of view, the application of an external magnetic field can lower their Gibbs free energies and thus change their formation sequence. Some calculated results have shown that the magnetization of χ-Fe$_5$C$_2$ is lower than that of η-Fe$_2$C at 200°C, as displayed in Fig. 11 [29]. Therefore, the total Gibbs free energy of χ-Fe$_5$C$_2$ may go lower than that of η-Fe$_2$C and it will precipitate before η-Fe$_2$C, as schematically illustrated in Fig. 12 [29].

4 Conclusions

The application of high magnetic fields can accelerate the austenite-to-ferrite transformation and increase the amount of ferrite. The two effects put together may produce a randomly distributed ferritic and pearlitic microstructure with an equilibrium amount of ferrite at a fast cooling rate of 46°C/min, which leads to an innovation to the conventional annealing method.

When the cooling rate is 10°C/min, the contribution of the applied magnetic fields in lowering the nucleation barrier and accelerating the transformation allows the ferrite to nucleate at higher temperatures. In this case, nucleation along austenite grain boundaries is dominant. Due to the inhomogeneous deformation of the previous hot rolling, the final microstructure of alternately distributed ferrite grains and pearlite colonies along the applied MD is obtained.

During high-temperature tempering, the applied 14-T magnetic field can effectively prevent the cementite from growing directionally along the plate and twin boundaries. Indeed, the magnetic field increases the cementite/ferrite interfacial energy and strain energy. Therefore, the formation of particle-like cementite is considered to be most energetically favorable. In addition, the magnetic field retards the recovery progress of the ferrite matrix, which may be attributed to the influence of magnetic ordering and domain walls on the diffusion and mobility of grain boundaries.

For low-temperature tempering, the magnetic field can change the precipitation sequence of transition carbides by changing their Gibbs free energies through magnetization. When tempered at 200°C for 60 min in a 14-T magnetic field, high-temperature monoclinic χ-Fe_5C_2 carbide is precipitated, as compared with the usual orthorhombic η-Fe_2C carbide formed without the magnetic field.

References

1. Krivoglaz M. -A. and Sadovskiy V. -D., Effect of strong magnetic fields on phase transformations, Fiz. Met. Metalloved., 1964, 4: 23–27
2. Bernshteyn M. -L., Granik G. -I. and Dolzhanskiy P. -R., Effect of magnetic field on the phase transformations in nickel steels, Fiz. Met. Metalloved., 1965, 6: 77–83
3. Voronchikhin L. -V. and Fakidov I. -G., Determining the latent heat of the martensitic transformation induced by a magnetic field in steel, Fiz. Met. Metalloved., 1966, 3: 119–124
4. Malinen P. -A. and Sadovskiy V. -D., Effect of a magnetic field on the $\alpha \rightarrow \gamma$ transformation in iron–nickel alloys, Fiz. Met. Metalloved., 1966, 5: 139–140
5. Satyanarayan K. -R., Eliasz W. and Miodownik A. -P., The effect of a magnetic field on the martensite transformation in steels, Acta Metall., 1968, 16: 877–887
6. Kakeshita T., Shimizu K., Maki T., Tamura I., Kijima S. and Date M., Magnetoelastic martensitic transformation in an ausaged Fe–Ni–Co–Ti alloy, Scr. Metall., 1985, 8: 973–976
7. Kakeshita T., Shimizu K., Funada S. and Date M., Composition dependence of magnetic field-induced martensitic transformations in Fe–Ni alloys, Acta Metall., 1985, 8: 1381–1389
8. Kakeshita T., Shimizu K., Ono M. and Date M., Magnetic field-induced martensitic transformations in a few ferrous alloys, J. Magn. Magn. Mater., 1990, 90–91: 34–36
9. Kakeshita T., Yamamoto T., Shimizu K., Sugiyama K. and Endo S., Effects of static magnetic field and hydrostatic pressure on the isothermal martensitic transformation in a Fe–Ni–Mn alloys, Mater. Trans., JIM, 1995, 8: 1018–1022
10. Kakeshita T., Saburi T. and Shimizu K., Effects of hydrostatic pressure and magnetic field on martensitic transformations, Mater. Sci. Eng., 1999, A273–275: 21–29
11. Shimozono T., Kohno Y., Konishi H., Shibata K., Ohtsuka H. and Wada H., Effect of pre-strain, heat treatments and magnetic fields on α' martensite formation in Fe-25.5%Ni-3–5%Cr alloys, Mater. Sci. Eng., 1999, 12: 337–341
12. Kurita Y., Emura S., Fujita K., Nagai K., Ishikawa K. and Shibata K., Effect of magnetic field on martenistic transformation and serration of austenitic Fe–Ni and Fe–Cr–Ni steels at 4 K, Fusion Eng. Des., 1993, 1: 445–450
13. Koyano T., Ikeda H., Yoshizaki R., Uehara K., Tasaki A., Ohtsuka H., Takamasu T., Wada H., Kido G. and Ohba T., Effect of magnetic field on $\gamma \rightarrow \alpha'$ martensitic transformation and magnetization of α' and α'' iron-nitrides, Mater. Trans., JIM, 2000, 8: 923–927
14. Shibata K., Shimozono T., Kohno Y. and Ohtsuka H., Effects of heat treatment, pre-strain and magnetic field on the formation of α' martensite in Fe-25.5Ni-4Cr and 304L steels, Mater. Trans., JIM, 2000, 8: 893–901
15. Joo H. -D., Kim S. -U., Shin N. -S. and Koo Y. -M., An effect of high magnetic field on phase transformation in Fe–C system, Mater. Lett., 2000, 5–6: 225–229
16. Guo H. and Enomoto M., Influence of magnetic fields on α/γ equilibrium in Fe–C (–X) alloys, Mater. Trans., JIM, 2000, 8: 911–916
17. Shimotomai M. and Maruta K., Aligned two-phase structures in Fe–C alloys, Scr. Mater., 2000, 5: 499–503
18. Ohtsuka H., Xu Y. and Wada H., Alignment of ferrite of grains during austenite to ferrite transformation in a high magnetic field, Mater. Trans., JIM, 2000, 8: 907–910
19. Shimotomai M., Maruta K., Mine K. and Matsui M., Formation of aligned two-phase microstructure by applying a magnetic field during the austenite to ferrite transformation in steels, Acta Mater., 2003, 10: 2921–2932
20. Choi J.-K., Ohtsuka H., Xu Y. and Choo W. -Y., Effects of a strong magnetic field on the phase stability of plain carbon steels, Scr. Mater., 2000, 3: 221–226
21. Ohtuska H., Xu Y., Choi J. -K., Oishi Y., Murai Y. and Wada H., Effect of high magnetic field on diffusional transformation behavior and structure, Proc. of the International Conference on Solid-Solid Phase Transformations '99 (JIMIC-3), Kyoto Park Hotel, The Japan Institute of Metals, 1999, 393–396
22. Xu Y., Ohtsuka H. and Wada H., Effect of high magnetic field on pearlite transformation behavior and structure, Trans. Mater. Res. Soc. Jpn., 2000, 25: 509–512
23. Enomoto M., Guo H., Tazuke Y., Abe Y. -R. and Shimotomai M., Influence of magnetic field on the kinetics of proeutectoid ferrite transformation in iron alloy, Metall. Mater. Trans., 2001, 3: 445–453
24. Zhang Y. -D., He C. -S., Zhao X., Zuo L., Esling C. and He J. C., Thermodynamic and kinetic characteristics of high temperature cooling phase transformation under high magnetic field, J. Magn. Magn. Mater. 2005, 3: 267–272
25. Zhang Y. -D., He C. -S., Zhao X., Zuo L. and Esling C., New phase equilibrium in Fe–C binary system under a magnetic field, Solid State Phenom., 2005, 105: 187–182
26. Zhang Y. -D., He C. S., Zhao X., Esling C. and Zuo L., A new approach for rapid annealing of medium carbon steels, Adv. Eng. Mater., 2004, 6: 310–313
27. Zhang Y. -D., He C. S., Zhao X., Zuo L., Esling C. and He J. -C., New microstructural features occurring during transformation from austenite to ferrite under kinetic influence of magnetic field in a medium carbon steel, J. Magn. Magn. Mater., 2004, 284: 287–293
28. Zhang Y. -D., Gey N., He C. -S., Zhao X., Zuo L. and Esling C., High temperature tempering behaviors in a structural steel under high magnetic field, Acta Mater., 2004, 10: 3467–3474
29. Zhang Y. -D., Zhao X., Bozzolo N., He C. -S., Zuo L. and Esling C., Low temperature tempering behaviors in a structural steel under high magnetic field, ISIJ Int., 2005, 45: 913–919
30. Zhang Y. -D., Vincent G., Dewobroto N., Germain L., Zhao X., Zuo L. and Esling C., The effect of thermal processing in a magnetic field on grain boundary characters of ferrite in a medium carbon steel, J. Mater. Sci., 2005, 40: 905–908
31. Chang H. -B., Li Z. -G., Hsu T. -Y. and Ruan X. -Y., Theoretical prediction of proeutectoid ferritic transformation in hypo-proeutectoid structure steels, Acta Metall. Sin. (Eng. Lett.), 1998, 3: 207–214
32. Hsu T. -Y., Theory of Phase Transformation, Beijing: Science Press of China, 1988, 35–43
33. Martikainen H. -O. and Lindroos V. -K., Observation on the effect of magnetic field on the recrystallization in ferrite, Scand. J. Metal., 1981, 10: 3–8
34. Krauss G., Principles of Heat Treatment of Steel, Ohio: American Society for Metals, 1980, 200–209